

Electronic Supporting Information

Bisphosphonate Ligand Mediated Ultrasensitive Capacitive Protein Sensor: Complementary Match of Supramolecular and Dynamic Chemistry

Gizem Ertürk^{a,b}, Maedeh Akhoundian^a, Kyra Lueg-Althoff^d, Sudhirkumar Shinde^{a,e†*}, Sing Yee Yeung^a, Martin Hedström^{b,c}, Thomas Schrader^{d#}, Bo Mattiasson^{b,c#}, Börje Sellergren^{a#}

^a Department of Biomedical Sciences, Faculty of Health and Society, Malmö University, SE-20506 Malmö, Sweden *Email: sudhirkumar.shinde@mah.se or s.shinde@qub.ac.uk

^b CapSenze Biosystems AB, Lund, 223 63, Sweden

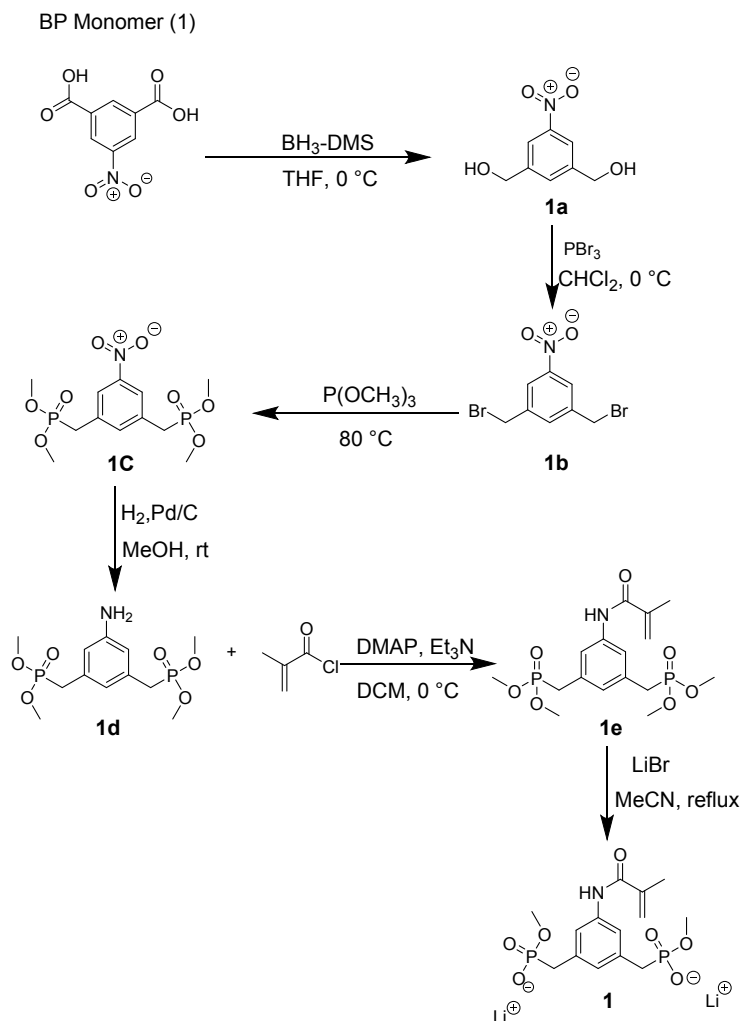
^c Department of Biotechnology, Lund University, Lund, 223 62, Sweden.

^d Department of Chemistry, University of Duisburg-Essen, Universitätsst. 7, 45117, Essen Germany

^e Current address: School of Chemistry and Chemical Engineering, Queens University Belfast, Northern Ireland

Table of Contents

| | |
|--|---------------|
| Scheme 1 Synthesis of functional monomer | Page S3 |
| Synthesis of functional monomer (BP, 1) | Page S3-S5 |
| Fig. S1 Cyclic voltammetry for monitoring the insulating effect of..... | Page S5 |
| Fig. S2 Scanning Electronic Microscopic (SEM) images of MIP and..... | Page S6 |
| Fig. S3 Atomic Force Microscopy (AFM) images of MIP capacitive..... | Page S6 |
| Fig. S4 Schematic diagram showing the capacitive sensor with automated..... | Page S7 |
| Fig. S5 Selectivity of trypsin-imprinted capacitive biosensor based on BP monomer | Page S7 |
| Table S1 Selectivity coefficients of trypsin-MIP and NIP electrode | Page S7 – S8 |
| Table S2 contact angle changes of stamp and gold sensor | Page S8 |
| Table S3 Comparison of analytical performances of different techniques.... | Page S8 – S9 |
| ¹ H, ¹³ C, ³¹ P NMR Spectra's of Compounds 1a, 1b, 1c, 1d, 1e1 (BP) | Page S9 – S17 |
| References | Page S17 |

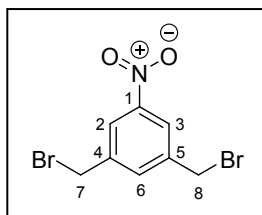


Scheme 1. Synthesis of 5-(Methacryloylamino)-m-xylylene bisphosphonic acid dimethylesterdilithium salt (**1**, BP) monomers

Synthesis of Functional Monomer

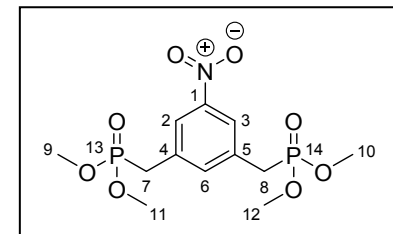
3, 5-bis - (hydroxymethyl) nitroxylylene (1a) 10 g of 5-nitroisophthalic acid (47.36 mmol, 1.0 equivalent) was dissolved in 100 mL dry THF and the mixture was cooled to 0 °C. 94.72 mL borane dimethyl sulfide complex solution (2.0 M $\text{BH}_3\text{-DMS}$ in THF) (14.39 g, 189.44 mmol, 4 equivalent) was then added dropwise using dropping funnel to the reaction mixture under argon atmosphere. The resulting reaction was stirred at 0 °C for 1 hr and left to stir for additional 48 h at room temperature. The unreacted borane complex was neutralized by dropwise addition of 100 mL methanol. After the removal of excess solvent, the yellow oily residue was dissolved in 500 mL ethyl acetate and washed with 100 mL saturated NaHCO_3 , water and brine respectively. The organic layer was dried with MgSO_4 and then solvent was removed by using rotavap. The crude compound **1a** was purified using silica gel column chromatography with a mixture of ethyl acetate: cyclohexane/ 5:1 gives (5.65 g, 81% yield) **1a** as pale-yellow crystals was obtained. $^1\text{H-NMR}$ (600 MHz, $\text{MeOD-}d_4$) δ [ppm] = **8.14** (s, 2H, H-2; H-3), **7.72** (s, 1H, H-6), **4.72** (s, 4H, H-8, H-9). $^{13}\text{C-NMR}$ (150.92 MHz, $\text{MeOD-}d_4$) δ [ppm] = **149.92** (C-1), **145.48** (C-4, C-5), **131.67** (C-6), **120.88** (C-2, C-3), **63.94** (C-8, C-9).

3, 5-bis-(bromomethyl) nitroxylylene (1b) 5.0 g of 3, 5-bis-(hydroxymethyl) nitroxylylene **1a** (27.3 mmol, 1 equivalent) was dissolved in 30 mL dry dichloromethane and cooled to 0 °C. To this solution, 6.5 mL (69.2 mmol, 2.5 equivalent) of phosphorus tribromide in 10 mL dry dichloromethane was added dropwise. The reaction

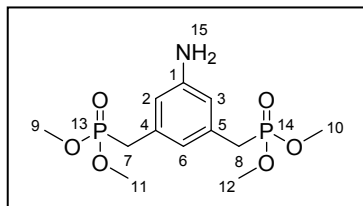


mixture was stirred for 1 h at 0 °C and then stirred for 3 days at room temperature. The resulting solution was poured into 200 g of crushed ice to neutralize the remaining phosphorus tribromide. The resulting suspension was then extracted with (4 x 100 mL) diethyl ether. The collected organic layers were washed twice with 50 mL saturated NaHCO₃, water and brine respectively. The organic layer was then dried with Na₂SO₄ and the excess ether was removed *in vacuo* to give (7.46 g, 91 % yield) **1b** as a pale-yellow powder. ¹H-NMR (600 MHz, CDCl₃) δ [ppm] = **8.19** (s, 2H, H-2; H-3), **7.75** (s, 1H, H-6), **4.52** (s, 4H, H-8, H-9). ¹³C-NMR (150.92 MHz, CDCl₃) δ [ppm] = **148.45** (C-1), **140.30** (C-4, C-5), **135.19** (C-6), **123.61** (C-2, C-3), **30.57** (C-7, C-8).

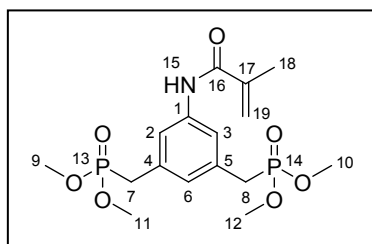
5-Nitro-*m*-xylylene bisphosphonic acid tetramethylester (1c) 5.1 g (16.5 mmol, 1 equivalent) of 3, 5-bis-(bromomethyl) nitro-xylylene (**1b**) was dissolved in 15 mL (127 mmol, 7.7 equivalent) trimethylphosphite. This solution was stirred for 5 h at 80 °C and was further stirred overnight at room temperature. The excessive trimethylphosphite was removed via condensation. The residue was dissolved in cyclohexane and stirred for 1 h. The obtained solid was filtered and recrystallized in hexane/ethyl acetate mixture to give (5.4 g; 89% yield) **1c** as solid compound. ¹H-NMR (600 MHz, CDCl₃) δ [ppm] = **8.03** (s, 2H, H-2; H-3), **7.59** (s, 1H, H-6), **3.71** (d, ³J = 10.9 Hz, 12H, H-9, H-10, H-11, H-12), **3.23** (d, ²J = 22.0 Hz, 4H, H-7, H-8). ¹³C-NMR (150.92 MHz, CDCl₃) δ [ppm] = **148.42** (C-1), **136.98** (C-4, C-5), **133.84** (C-2, C-3), **123.19** (C-6), **53.00** (C-9, C-10, C-11, C-12), **32.43** (d, *J*_{C,P} = 138.9 Hz, C-7, C-8). ³¹P-NMR (242.92 MHz, CDCl₃) δ [ppm] = **26.80** (P-13, P-14).



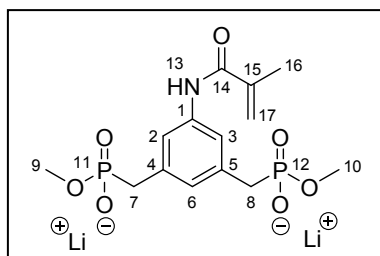
5-Amino-*m*-xylylene bisphosphonic acid tetramethyl ester (1d) 0.45 g (1.27 mmol, 1 equivalent) of 5-Nitro-*m*-xylylene bisphosphonic acid tetramethylester (**1c**) and 12 mg of palladium on Carbon was dispersed in 20 mL absolute ethanol. The hydrogen gas was placed into reaction vessel by flushing and the reaction mixture was stirred for two days at room temperature. The Pd/C was removed via filtration over celite before the solvent was removed *in vacuo* to give the product **1d** (0.4 g, 97% yield) was a white solid. ¹H-NMR (600 MHz, CDCl₃) δ [ppm] = **6.61** (s, 1H, H-6), **6.58** (s, 2H, H-2; H-3), **4.14** (bs, 2H, H-15), **3.66** (d, ³J = 10.8 Hz, 12H, H-9, H-10, H-11, H-12), **3.04** (d, ²J = 21.8 Hz, 4H, H-7, H-8). ¹³C-NMR (150.92 MHz, CDCl₃) δ [ppm] = **146.09** (C-1), **132.17** (C-4, C-5), **122.06** (C-2, C-3), **115.87** (C-6), **53.06** (C-9, C-10, C-11, C-12), **32.76** (d, *J*_{C,P} = 138.1 Hz, C-7, C-8). ³¹P-NMR (242.92 MHz, CDCl₃) δ [ppm] = **26.86** (P-13, P-14).



5-(Methacryloylamino)-*m*-xylylenebisphosphonic acid tetramethylester (1e) 2.05 g (6.1 mmol, 1 equivalent) of 5-Amino-*m*-xylylene bisphosphonic acid tetramethylester (**1d**), 0.95 mL (0.69 g, 6.8 mmol, 1.1 equivalent) triethylamine and a catalytic amount of 4-(*N,N*-dimethylamino)-pyridine was dissolved in 50 mL dry dichloromethane. A solution of 0.88 mL (0.95 g, 9.1 mmol, 1.5 equivalent) methacryloyl chloride in 20 mL dry dichloromethane was added dropwise at 0 °C within 1 h. The reaction mixture was stirred for an additional hour at room temperature. The reaction mixture was washed several times with 0.6 M NaOH and then dried with anhydrous Na₂SO₄. The solvent was evaporated in vacuum oven. The crude product was purified by silica gel column chromatography with dichloromethane/methanol 19:1 solvent mixture and the obtained product **1e** (1.4 g, 57 % yield) was yellow oil. ¹H-NMR (600 MHz, CDCl₃) δ [ppm] = **7.89** (s, 1H, H-15), **7.44** (s, 2H, H-2, H-3), **6.94** (s, 1H, H-6), **5.77** (s, 1H, H-19a), **5.42** (s, 1H, H-19b), **3.65** (d, ³J = 10.8 Hz, 12H, H-9, H-10, H-11, H-12), **3.09** (d, ²J = 21.9 Hz, 4H, H-7, H-8), **2.00** (s, 3H, H-18). ¹³C-NMR (150.92 MHz, CDCl₃) δ [ppm] = **166.72** (C-16), **140.48** (C-17), **138.49** (C-1), **132.16** (C-4, C-5), **126.66** (C-6), **120.04** (C-19), **119.98** (C-2, C-3), **52.86** (C-9, C-10, C-11, C-12), **32.38** (d, *J*_{C,P} = 137.9 Hz, C-7, C-8), **18.60** (C-18). ³¹P-NMR (242.92 MHz, CDCl₃) δ [ppm] = **26.28** (P-13, P-14).



5-(Methacryloylamino)-*m*-xylylenebisphosphonic acid dimethylester dilithium salt (BP; 1) 1.05 g (2.59 mmol, 1 equivalent) of 5-(Methacryloylamino)-*m*-xylylenebisphosphonic acid tetramethylester (**1e**) was dissolved in 50 mL absolute acetonitrile. To the solution 655 mg (7.54 mmol, 2.9 equivalent) of Lithium Bromide was added and the reaction mixture was refluxed overnight. The resulting



reaction mixture was centrifuged to recover the solid pellet. The pellet was washed with (4 x 15 mL) diethyl ether and dried *in vacuo* to gave (0.97 g, 96 % yield) off-white solid product (**1**). ¹H-NMR (600 MHz, D₂O) δ [ppm] = **7.22** (s, 2H, H-2, H-3), **7.05** (s, 1H, H-6), **5.81** (s, 1H, H-17a), **5.56** (s, 1H, H-17b), **3.54** (d, ³J = 10.3 Hz, 6H, H-9, H-10), **3.04** (d, ²J = 20.4 Hz, 4H, H-7, H-8), **2.01** (s, 3H, H-16). ¹³C-NMR (150.92 MHz, D₂O) δ [ppm] = **173.46** (C-14), **142.26** (C-15), **139.21** (C-1), **138.19** (C-4, C-5), **130.61** (C-6), **124.04** (C-19), **124.00** (C-2, C-3), **54.36** (d, ²J_{C,P} = 6.0 Hz, C-9, C-10), **35.87** (d, J_{C,P} = 129.4 Hz, C-7, C-8), **20.30** (C-16). ³¹P-NMR (242.92 MHz, D₂O) δ [ppm] = **26.31** (P-11, P-12).

HRMS (pos. APCI, MeOH): Calculated for C₁₄H₂₁NO₇P₂, M+nH: 378.0866; Found: 378.0848.

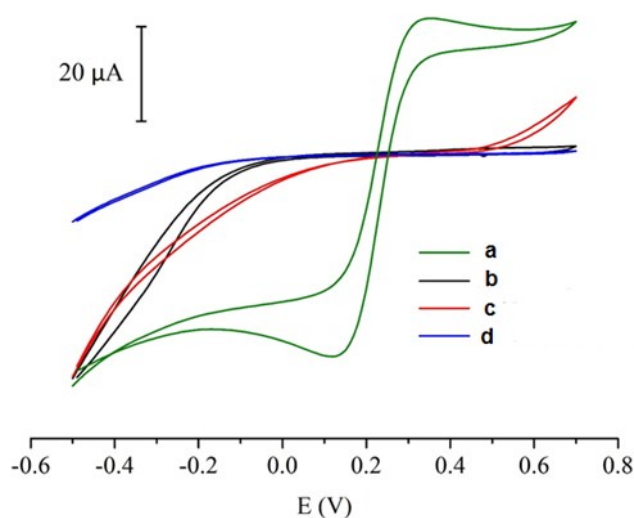


Fig. S1 Cyclic voltammetry for monitoring the insulating effect of the different modification steps on the gold electrode using ferro/ferricyanide solution. (a) Bare gold electrode; (b) gold electrode after electropolymerization of tyramine; (c) gold electrode after surface acryloyl chloride; (d) trypsin Imprinted electrode after treatment with 1-dodecanethiol. The scan range was from -0.5 V to +0.7 V (vs. Ag/AgCl) at scan rate of 0.1 Vs⁻¹.

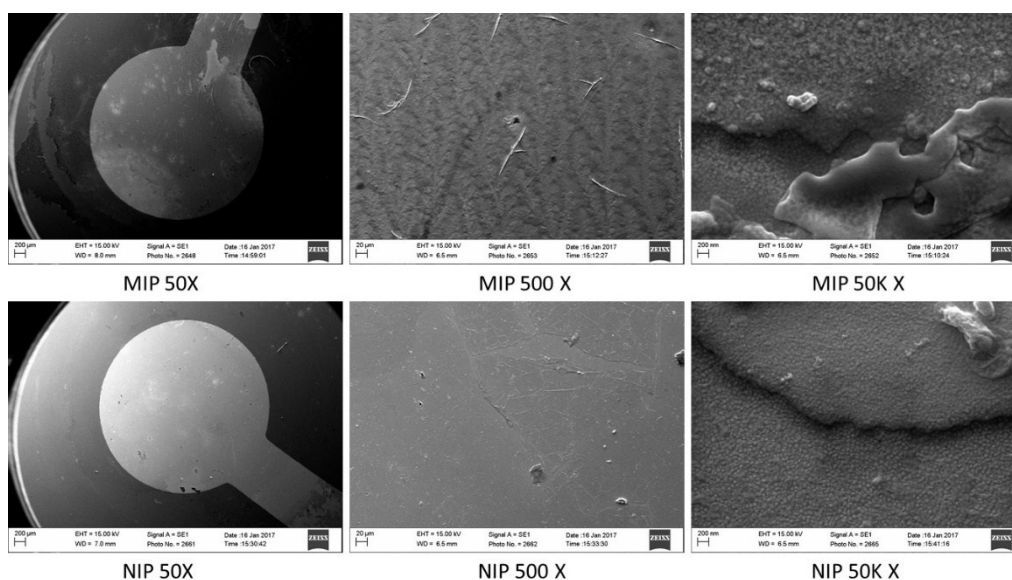


Fig. S2 Scanning electronic microscopic (SEM) images of MIP and NIP capacitive sensor surfaces at different magnifications.

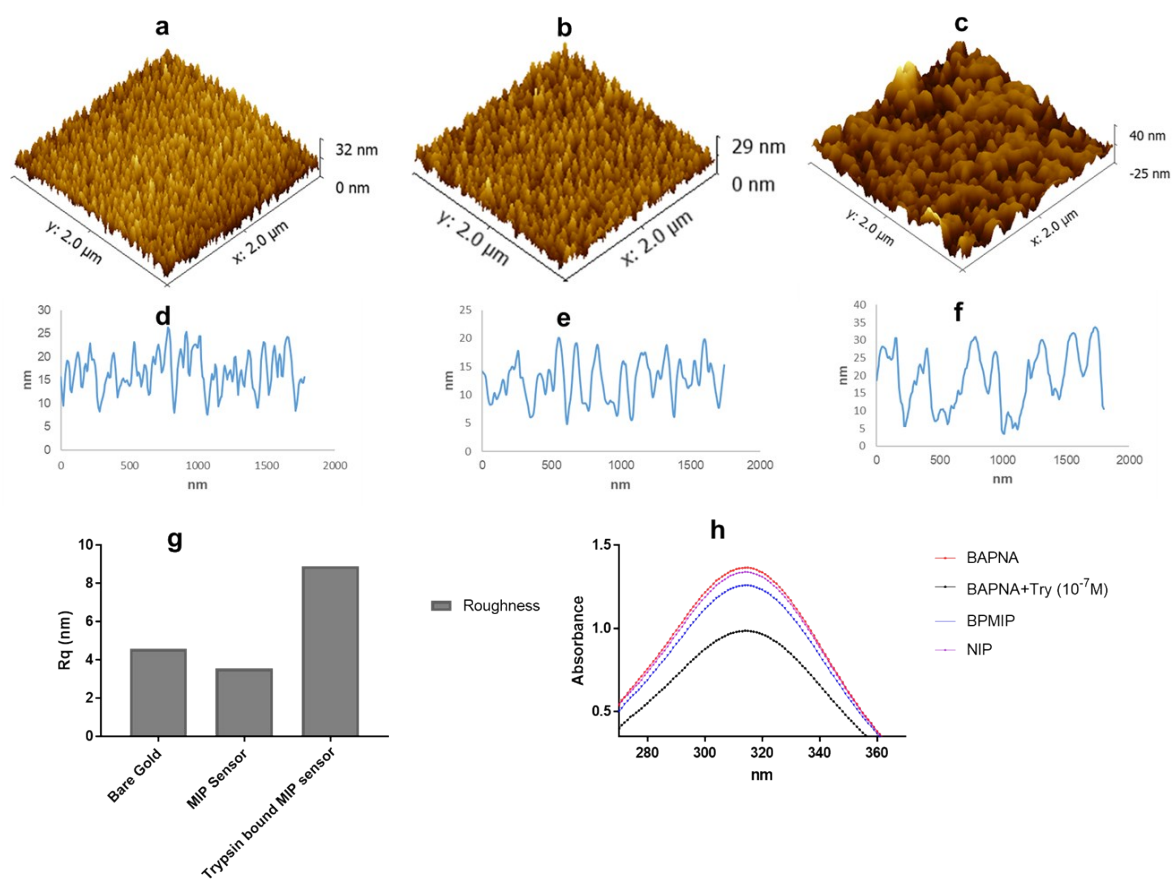


Fig. S3 Atomic Force Microscopic (AFM) images of capacitive sensor surfaces a) bare gold, b) MIP sensor, c) trypsin bound MIP sensor; d, e, f, g) roughness profile of bare gold electrode, MIP sensor, Trypsin bound MIP sensor; h) Enzyme activity of Trypsin bound MIP and NIP sensors.

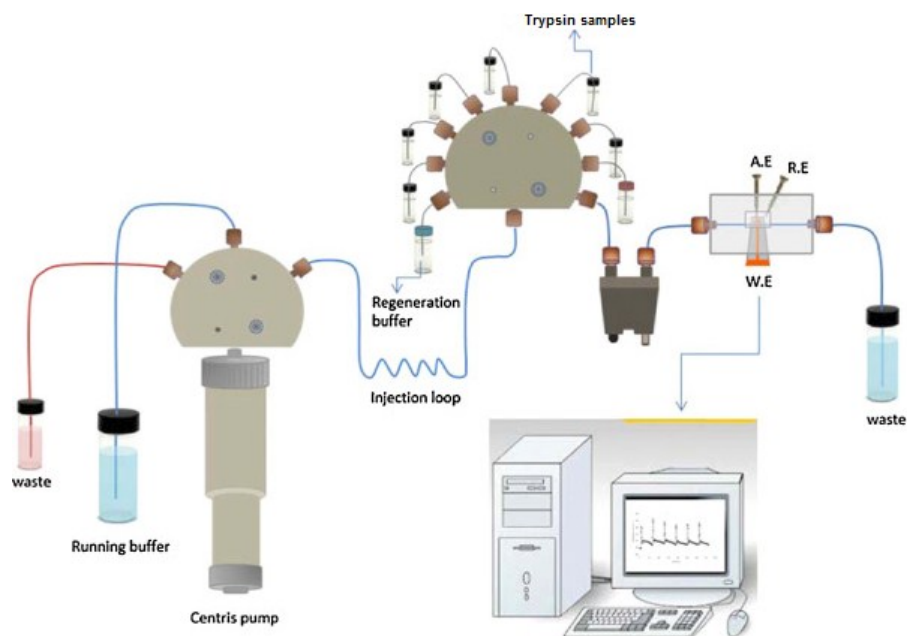


Fig. S4 Schematic diagram showing the capacitive sensor with an automated flow injection system¹.

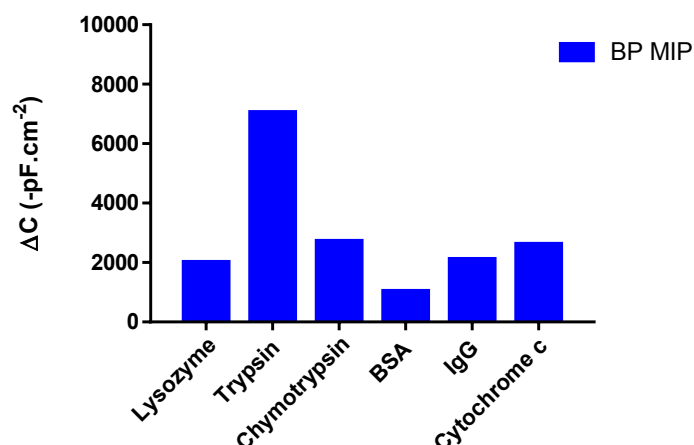


Fig. S5 Selectivity of Trypsin-imprinted capacitive biosensor based on BP monomer in 100 mM phosphate buffer pH 7.4 against competing proteins. Chymotrypsin (pI – 8.3, 25.6 KDa), Bovine Serum Albumin (pI – 5.8; 66.5 KDa), Cytochrome C (pI – 10.0±0.5; 12.3 KDa), Lysozyme (pI – 11.35; 14.3 KDa), IgG (pI – 6.85 ± 1; 155 – 160 KDa) and trypsin (pI – 10.1±0.5; 23.3 KDa) in singular manner Conditions: protein concentration 1.0 mg/mL (3.9×10^{-5} M for chy, 1.5×10^{-5} M for BSA, 7.0×10^{-5} M for lyz and 8.1×10^{-5} M for cyt c, 4.3×10^{-5} M for try).

Table S1. Selectivity coefficients of trypsin-MIP and NIP electrode

| Functional Monomer (FM) | Proteins | ΔC (pF) MIP | ΔC (pF) NIP | Selectivity coefficient k (MIP) | Selectivity coefficient k (NIP) | Relative selectivity coefficient (k') |
|-------------------------|--------------|-------------|-------------|---------------------------------|---------------------------------|---------------------------------------|
| BP | Lysozyme | 3947 | 1544 | 4.0 | 2.48 | 1.63 |
| | Trypsin | 15920 | 3822 | - | - | - |
| | Chymotrypsin | 1539 | 3056 | 10.4 | 1.25 | 8.28 |
| | BSA | 2640 | 1522 | 6.0 | 2.51 | 2.41 |
| | IgG | 3851 | 2516 | 4.1 | 1.52 | 2.72 |
| | Cytochrome C | 3034 | 3631 | 5.3 | 1.05 | 4.99 |
| Without FM* | Lysozyme | 1128 | 2011 | 6.5 | 1.02 | 6.39 |
| | Trypsin | 7331 | 2044 | - | - | - |
| | Chymotrypsin | 10 | 1966 | 733.1 | 1.04 | 705.1 |
| | BSA | 694 | 1266 | 10.6 | 1.61 | 6.54 |
| | Cytochrome C | 2118 | 3014 | 3.5 | 0.68 | 5.10 |

Δ: capacitance change for the trypsin-MIP and NIP electrodes (BP as FM in 50 mM Phosphate Buffer pH: 7.4. K: selectivity coefficient for trypsin verses competing proteins, k': relative selectivity coefficient for trypsin-MIP electrode versus NIP electrode]. *: data was obtained in 10 mM phosphate buffer pH- 7.4 from our previous publication². The MIP electrode without functional monomer failed to perform in > 10 mM phosphate buffer (pH-7.4).

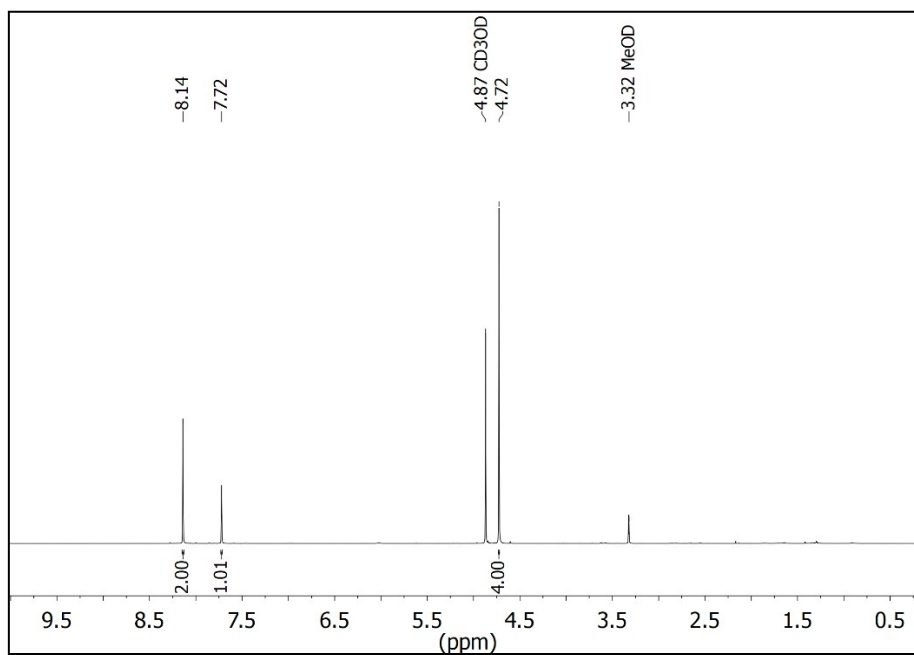
Table S2 Contact angle changes of stamp and gold sensor during modification step (measured in triplicates)

| Glass | WCA, ° | Gold electrode | WCA, ° |
|---------------------|------------|-----------------------|------------|
| Bare glass | 56.68±2.35 | Tyramine polymer | 66.27±1.85 |
| Acid/base treatment | 25.17±2.17 | Acryloyl modification | 53.77±2.54 |
| APTES Modified | 81.26±0.82 | After polymerization | 79.27±2.65 |
| GA-Modified | 74.98±1.11 | | |
| Trypsin Immobilized | 64.05±1.44 | | |
| After peeling off | 76.33±1.88 | | |

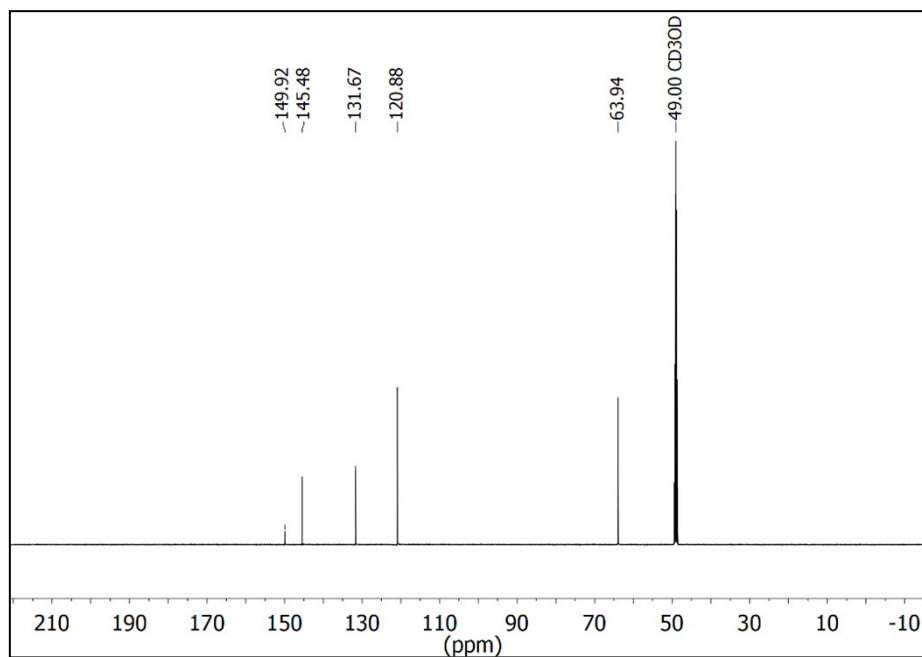
Table S3 Comparison of analytical performances of different techniques used for trypsin detection

| Sensing principle | Sensor preparation method | Limit of detection (LOD) | Ref |
|--|--|--------------------------|---------------------------------------|
| Colorimetric sensor | Employing cytochrome c as an enzyme substrate, 3,3',5,5'-tetramethylbenzidine as a chromogenic reagent | 1.9×10^{-10} M | Zhang and Du 2016 ³ |
| Liquid crystal (LC) sensor system | BSA immobilized gold grids as the enzymatic substrate | 4.3×10^{-10} M | Schyr et al. 2014 ⁴ |
| Interferometric sensor | Combination of chemically functionalized nanoporous anodic alumina photonic films and reflectometric interference spectroscopy | 1.07×10^{-6} M | Arredondo et al. 2012 ⁵ |
| Localized SPR | Integration of light weight and simple laboratory optical components with the camera module of the smartphone | 1.10×10^{-6} M | Dutta et al. 2016 ⁶ |
| Fluorescence detection system | Cell phone based portable bioassay platform | 3.9×10^{-11} M | Reddy et al. 2012 ⁷ |
| Flow injection analysis-QCM biosensors | Immobilizing trypsin inhibitor as a specific ligand | 0.16×10^{-6} M | Huang et al. 2015 ⁸ |
| Turn-on chemiluminescent biosensing platform | Using streptavidin-modified magnetic beads | 1.0×10^{-11} M | Zhang et al. 2014 ⁹ |
| Fluorescence based sensing | Functional high surface area scaffolds based on cellulose nanocrystals and polyvinyl alcohol | 10.7×10^{-6} M | Osman et al. 2013 ¹⁰ |
| Electrochemical immunosensor | Multiwall carbon nanotubes (MWCNTs)-composite modified electrode | 0.86×10^{-13} M | Yi et al. 2014 ¹¹ |
| Fluorescent sensors | Quantum-dot based | 0.42×10^{-9} M | Zhang et al. 2014 ¹² |
| QCM | Surface imprinting (molecular imprinting) | 43×10^{-10} M | Hayden et al. 2006 ¹³ |
| Square wave voltammetric sensor | 1,2-benzoquinone electrochemical reduction on gelatin coated screen printed electrodes | 4.3×10^{-10} M | Stoytcheva et al. 2012 ¹⁴ |
| Self-powered sensor | Signals the presence of trypsin via a light-emitting diode (LED) that is visible to the unaided eye | 2.1×10^{-8} M | Zaccheo and Crooks 2011 ¹⁵ |
| Amperometric sensor | Two layer configuration; a polymer-glucose oxidase inner layer and a gelatin outer layer | 42×10^{-12} M | Ionescu et al. 2006 ¹⁶ |

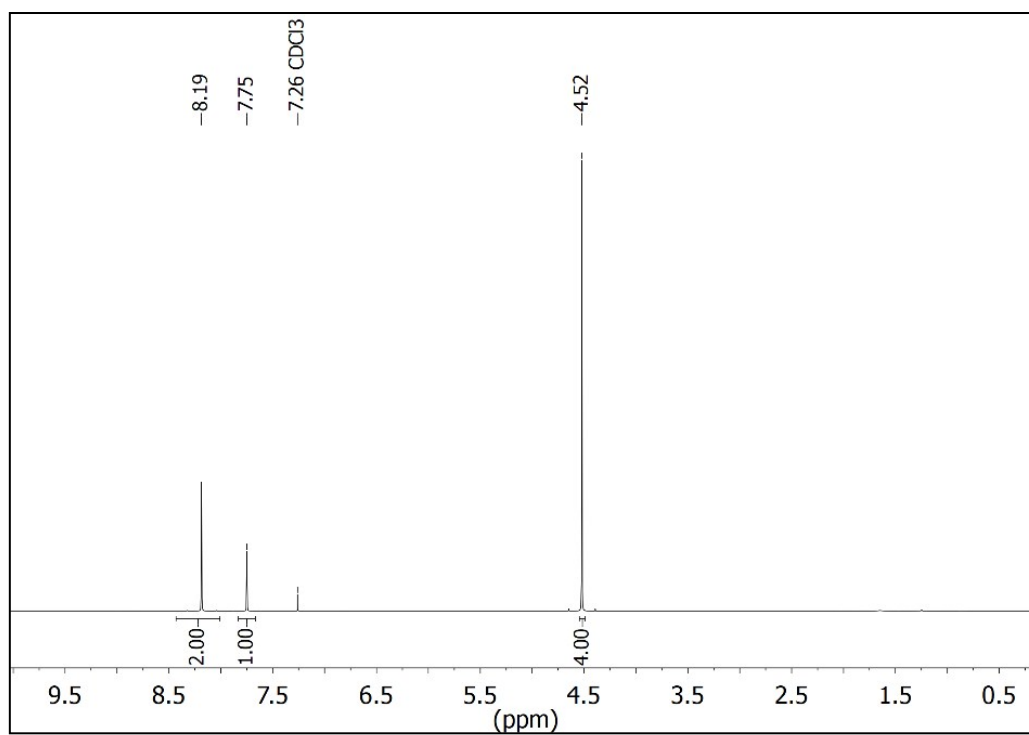
| | | | |
|------------------------|---|-------------------------|--|
| Electrochemical method | Gelatin coated glassy carbon electrode | 4.3×10^{-10} M | Tan and Wei 2015 ¹⁷ |
| Capacitive biosensor | Microcontact imprinting of trypsin to the electrode | 3.0×10^{-13} M | Ertürk and Mattiasson et al. 2016 ² |
| Capacitive biosensor | Microcontact imprinting of trypsin using bisphosphonate based functional monomer to the electrode | 1×10^{-13} M | In this study |



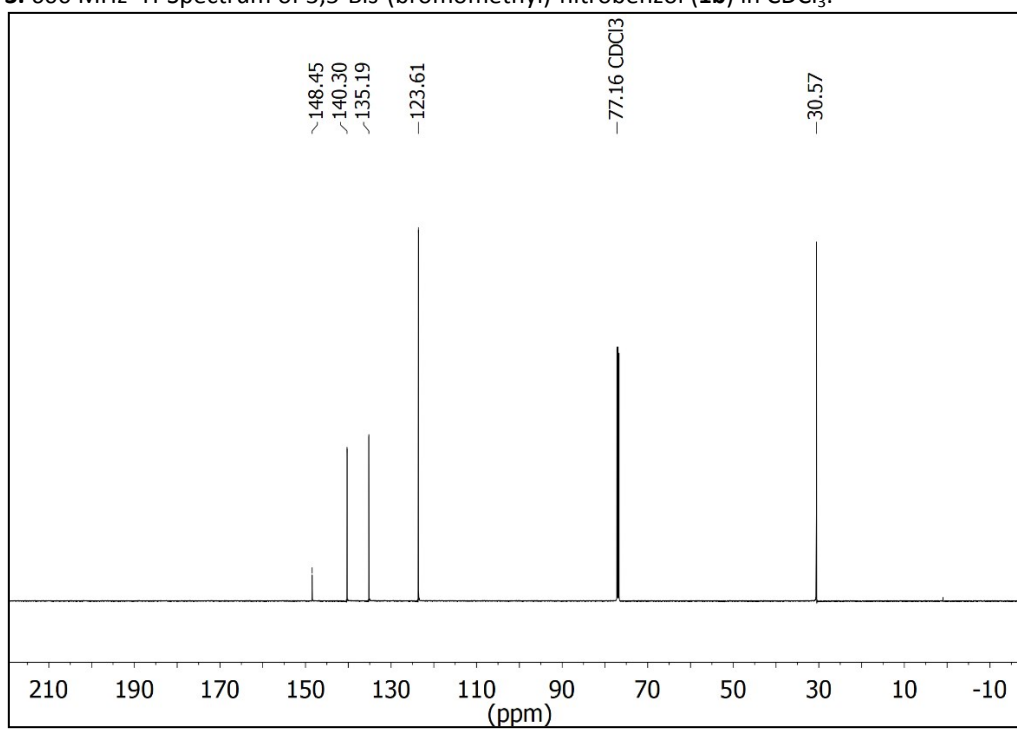
Spectra 1. 600 MHz ^1H -Spectrum of 3,5-Bis-(hydroxymethyl)-nitrobenzol (**1a**) in MeOD.



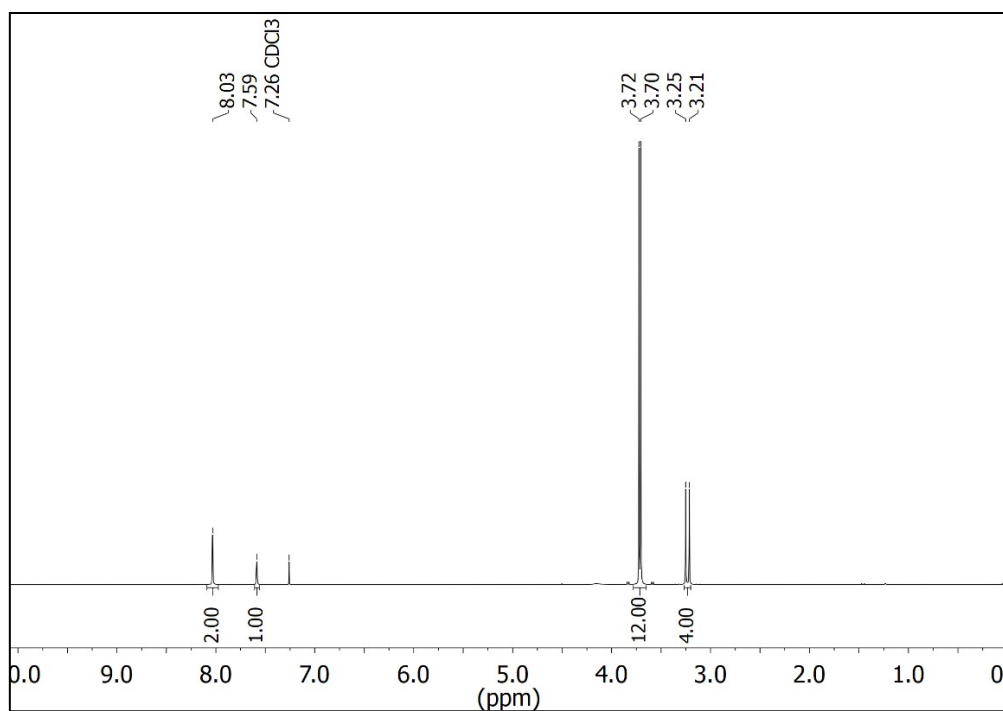
Spectra 2. 150.92 MHz ^{13}C -Spectrum of 3,5-Bis-(hydroxymethyl)-nitrobenzol (**1a**) in MeOD.



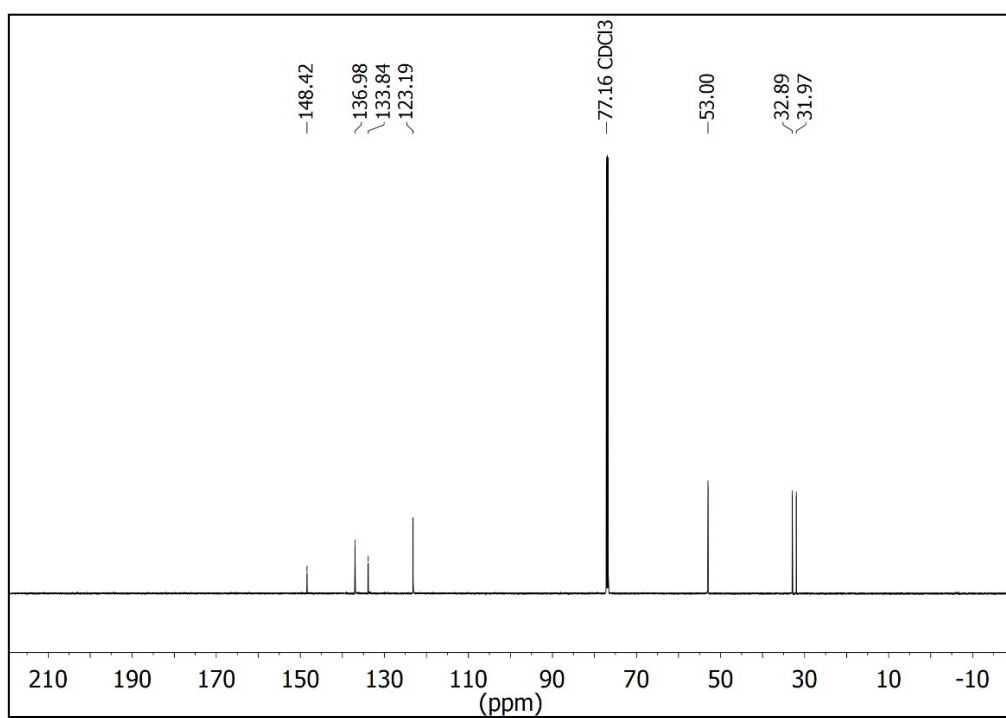
Spectra 3. 600 MHz ^1H -Spectrum of 3,5-Bis-(bromomethyl)-nitrobenzol (**1b**) in CDCl_3 .



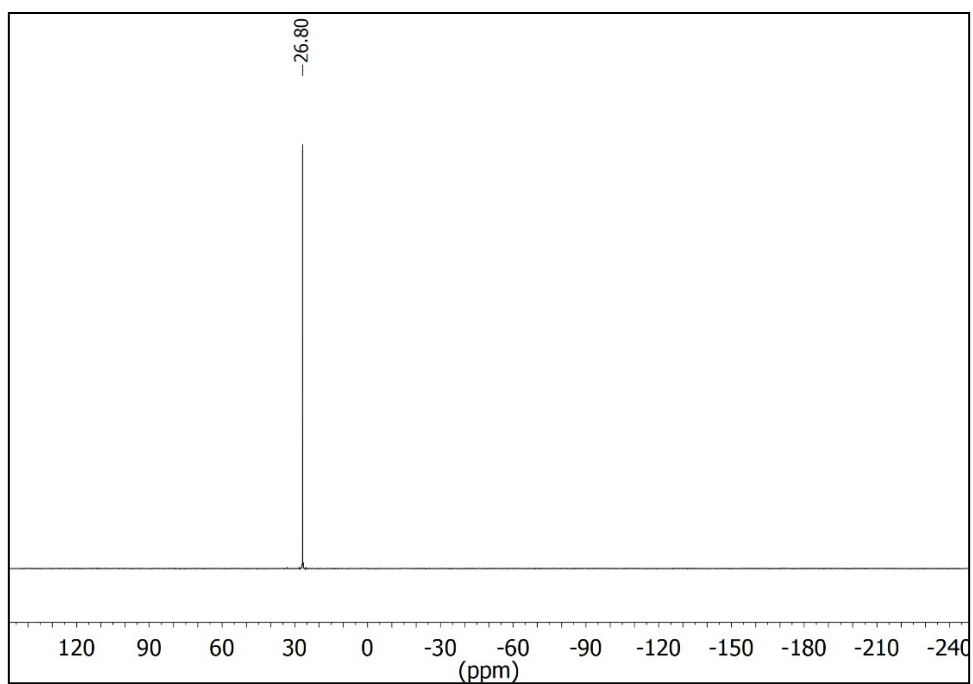
Spectra 4. 150.92 MHz ^{13}C -Spectrum of 3,5-Bis-(bromomethyl)-nitrobenzol (**1b**) in CDCl_3 .



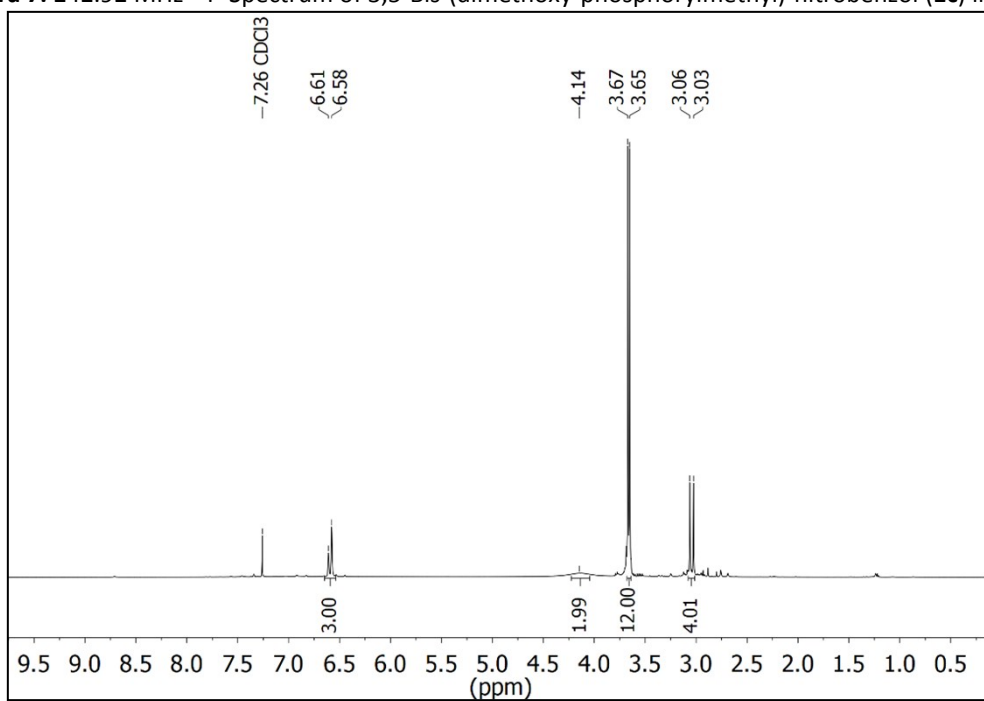
Spectra 5. 600 MHz ^1H -Spectrum of 3,5-Bis-(dimethoxy-phosphorylmethyl)-nitrobenzol (**1c**) in CDCl_3 .



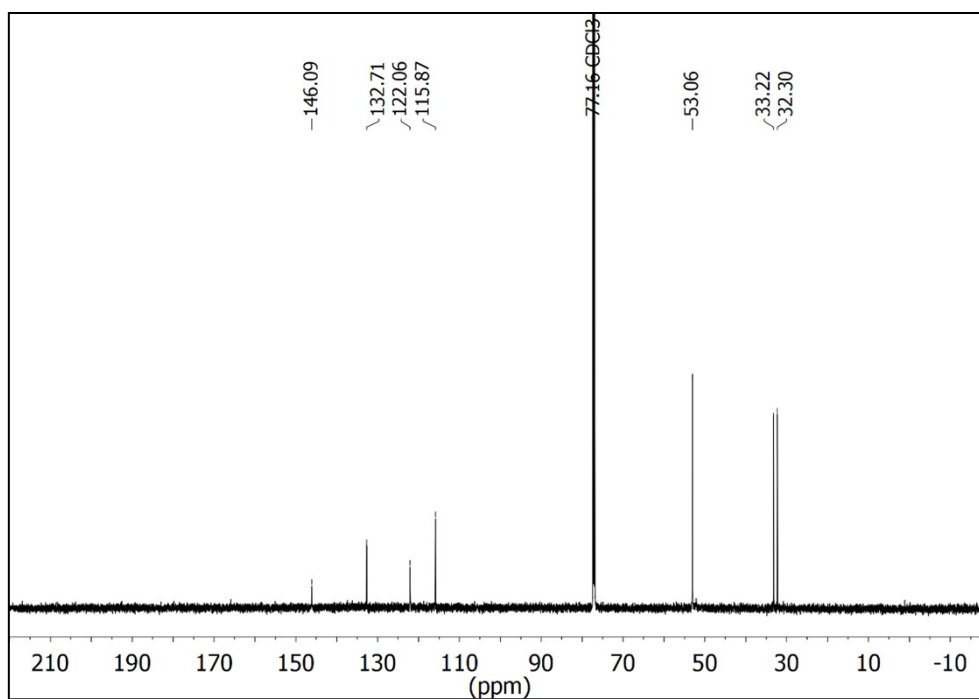
Spectra 6. 150.92 MHz ^{13}C -Spectrum of 3,5-Bis-(dimethoxy-phosphorylmethyl)-nitrobenzol (**1c**) in CDCl_3 .



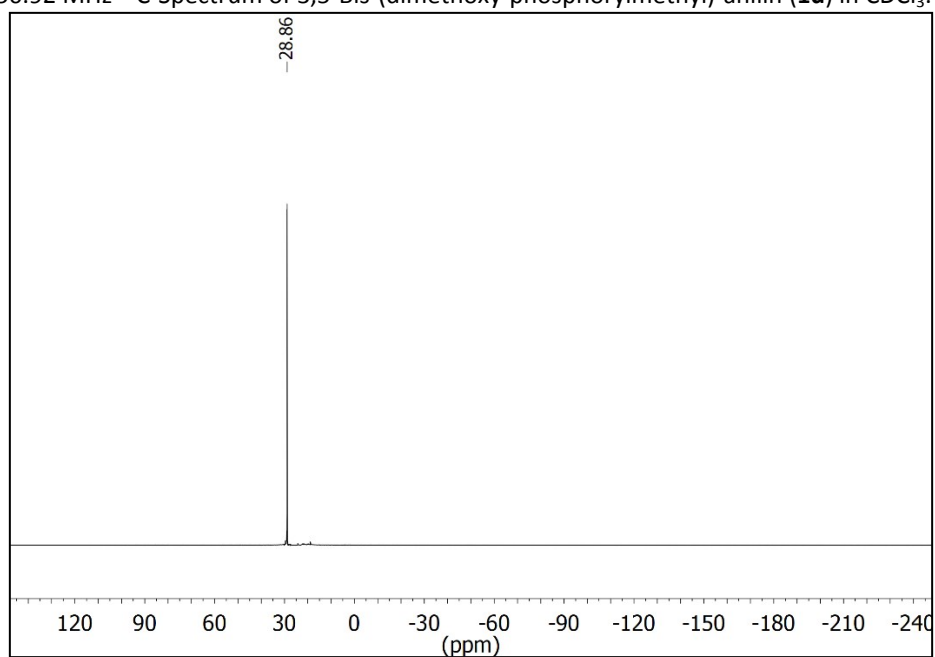
Spectra 7. 242.92 MHz ³¹P-Spectrum of 3,5-Bis-(dimethoxy-phosphorylmethyl)-nitrobenzol (**1c**) in CDCl₃.



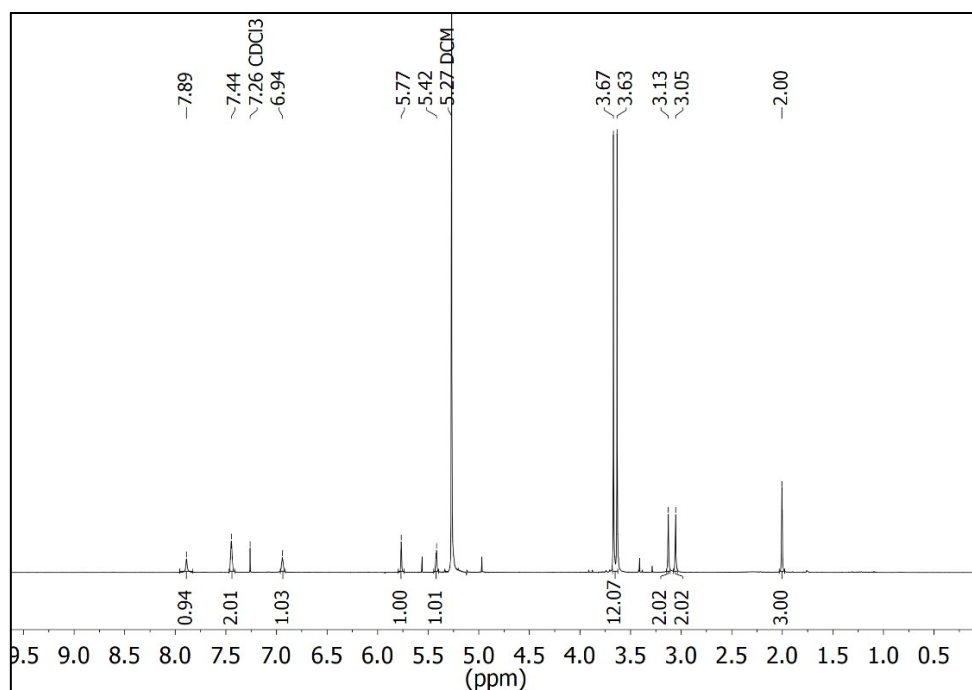
Spectra 8. 600 MHz ¹H-Spectrum of 3,5-Bis-(dimethoxy-phosphorylmethyl)-anilin (**1d**) in CDCl₃.



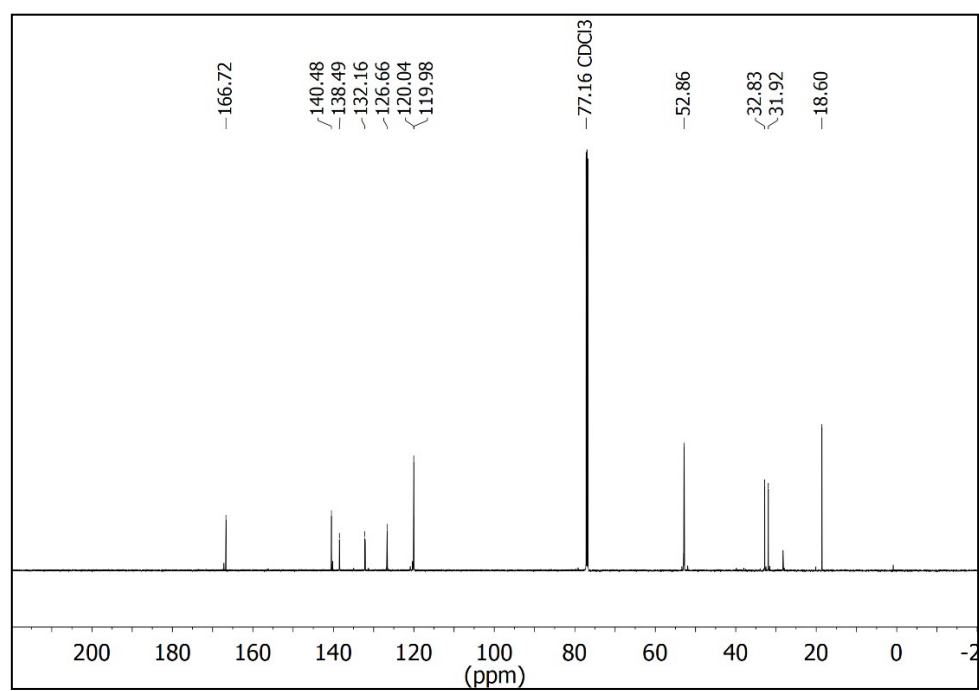
Spectra 9. 150.92 MHz ^{13}C -Spectrum of 3,5-Bis-(dimethoxy-phosphorylmethyl)-anilin (**1d**) in CDCl_3 .



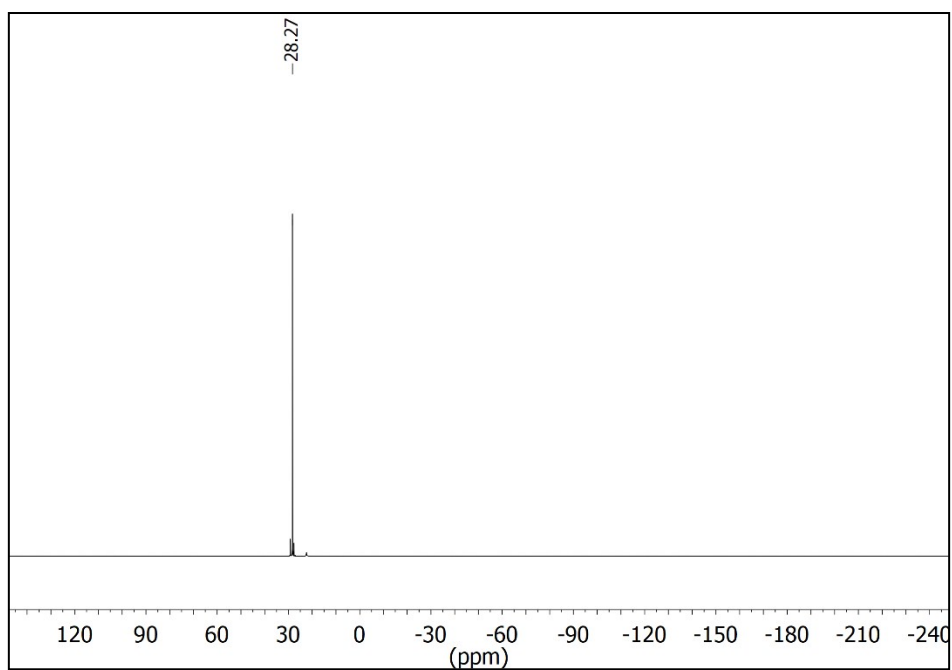
Spectra 10. 242.92 MHz ^{31}P -Spectrum of 3,5-Bis-(dimethoxy-phosphorylmethyl)-anilin (**1d**) in CDCl_3 .



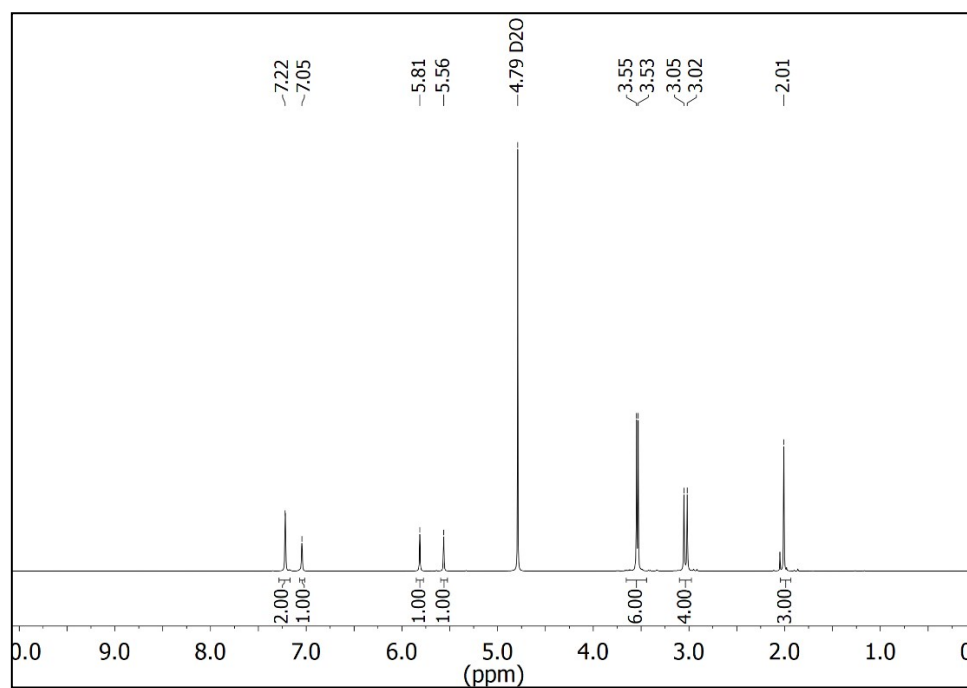
Spectra 11. 600 MHz ^1H -Spectrum of *N*-Methacryl-[3,5-Bis(dimethoxy-phosphorylmethyl)]-phenyl (**1e**) in CDCl_3 .



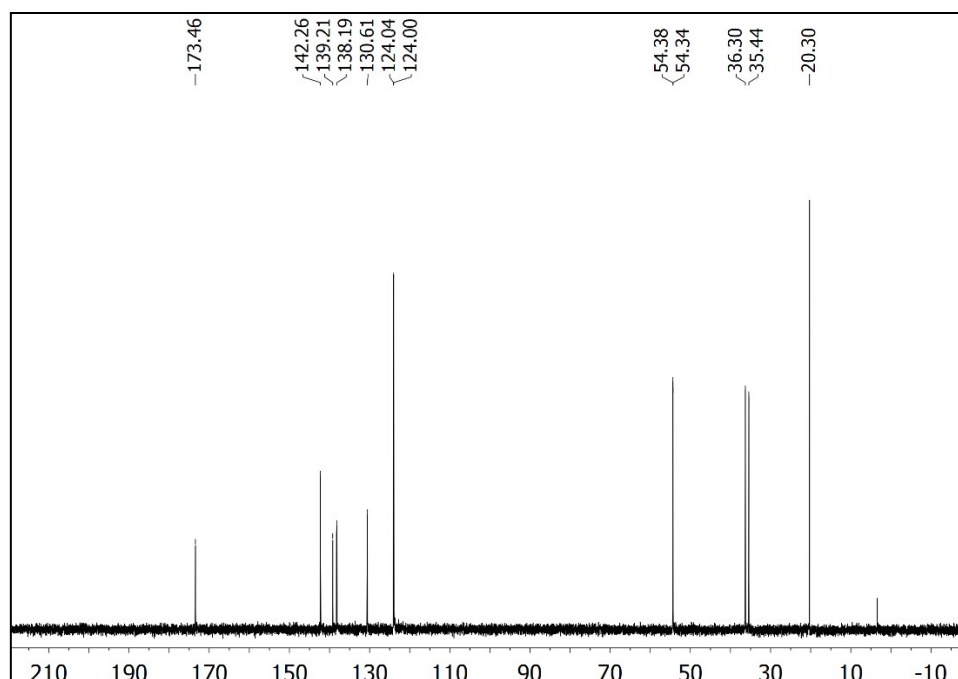
Spectra 12. 150.92 MHz ^{13}C -Spectrum of *N*-Methacryl-[3,5-Bis(dimethoxy-phosphorylmethyl)]-phenyl (**1e**) in CDCl_3 .



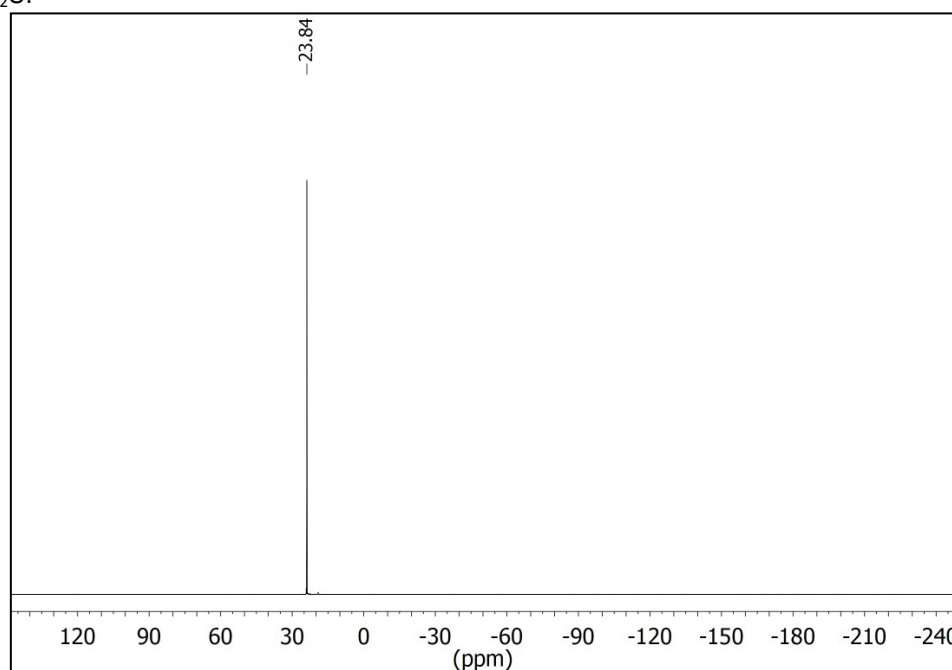
Spectra 13. 242.92 MHz ³¹P-Spectrum of *N*-Methacryl-[3,5-Bis(dimethoxy-phosphorylmethyl)]-phenyl (**1e**) in CDCl₃.



Spectra 14. 600 MHz ¹H-Spectrum of Dilithium-*N*-Methacryl-[3,5-Bis(methoxy-phosphorylmethyl)]-phenyl (**1**) in D₂O.



Spectra 15. 150.92 MHz ^{13}C -Spectrum of Dilithium-*N*-Methacryl-[3,5-Bis(methoxy-phosphorylmethyl)]-phenyl (BP, **1**) in D_2O .



Spectra 16. 242.92 MHz ^{31}P -Spectrum of Dilithium-*N*-Methacryl-[3,5-Bis(methoxy-phosphorylmethyl)]-phenyl (BP, **1**) in D_2O .

References

1. G. Ertürk, D. Berillo, M. Hedström and B. Mattiasson, *Biotechnology Reports*, 2014, **3**, 65-72.
2. G. Ertürk, M. Hedström and B. Mattiasson, *Biosensors and Bioelectronics*, 2016, **86**, 557-565.
3. L. Zhang and J. Du, *Biosensors and Bioelectronics*, 2016, **79**, 347-352.
4. B. Schyrr, S. Pasche, G. Voirin, C. Weder, Y. C. Simon and E. J. Foster, *ACS Applied Materials & Interfaces*, 2014, **6**, 12674-12683.
5. M. Arredondo, M. Stoytcheva, R. Zlatev and S. Cosnier, *ECS Electrochemistry Letters*, 2012, **1**, B1-B3.
6. S. Dutta, K. Saikia and P. Nath, *RSC Advances*, 2016, **6**, 21871-21880.

7. S. M. Reddy, Q. T. Phan, H. El-Sharif, L. Govada, D. Stevenson and N. E. Chayen, *Biomacromolecules*, 2012, **13**, 3959-3965.
8. Y. Huang, Q. Zhang, G. Liu and R. Zhao, *Chemical Communications*, 2015, **51**, 6601-6604.
9. H. Zhang, D. Yu, Y. Zhao and A. Fan, *Biosensors and Bioelectronics*, 2014, **61**, 45-50.
10. B. Osman, L. Uzun, N. Beşirli and A. Denizli, *Materials Science and Engineering: C*, 2013, **33**, 3609-3614.
11. Q. Yi, Q. Liu, F. Gao, Q. Chen and G. Wang, *Sensors*, 2014, **14**, 10203.
12. W. Zhang, P. Zhang, S. Zhang and C. Zhu, *Analytical Methods*, 2014, **6**, 2499-2505.
13. O. Hayden, C. Haderspock, S. Krassnig, X. Chen and F. L. Dickert, *Analyst*, 2006, **131**, 1044-1050.
14. M. Stoytcheva, R. Zlatev, S. Cosnier and M. Arredondo, *Electrochimica Acta*, 2012, **76**, 43-47.
15. B. A. Zaccaro and R. M. Crooks, *Analytical Chemistry*, 2011, **83**, 1185-1188.
16. R. E. Ionescu, S. Cosnier and R. S. Marks, *Analytical Chemistry*, 2006, **78**, 6327-6331.
17. Y. Tan and T. Wei, *Talanta*, 2015, **141**, 279-287.